

Thermal and Photolytic Reactions of Group 12 Metal Atoms in HCl-Doped Argon Matrixes: Formation and Characterization of the Hydride Species HMCl (M = Zn, Cd, or Hg)

Victoria A. Macrae,[†] Jennifer C. Green,[†] Tim M. Greene,^{*,‡} and Antony J. Downs[†]

Inorganic Chemistry Laboratory, University of Oxford, South Parks Road, Oxford, OX1 3QR, United Kingdom, and Department of Chemistry, University of Exeter, Stocker Road, Exeter, EX4 4QD, United Kingdom

Received: January 9, 2004

IR and UV–vis spectroscopic measurements have been used to chart the thermal and photolytic reactions occurring in HCl-doped Ar matrixes containing Zn, Cd, or Hg atoms (M). Following the formation of a loosely bound metal atom adduct $M\cdots\text{HCl}$, the primary reaction induced by UV irradiation ($200 \leq \lambda \leq 400$ nm) is insertion of M into the H–Cl bond to give the molecule HMCl, which has been characterized by its IR spectrum, with assignments validated by the effects of isotopic change (^1H , $^{35,37}\text{Cl}$, and $^{64,66,68}\text{Zn}$) and by the results of density functional theory calculations. The properties of HMCl are compared with those of other Group 12 metal hydrides, and the mechanism of insertion is also discussed.

I. Introduction

Although there exists, to our knowledge, no previous matrix-isolation study of the reaction between Zn or Cd atoms and HCl, several other metals have been investigated for their response to HCl. Thus, a more electropositive metal atom from Group 1 reacts to form the ion pair $M^+\text{HCl}^-$, which can be detected by its electron paramagnetic resonance (EPR) spectrum; this occurs spontaneously when $M = \text{K}$ but only on irradiation when $M = \text{Na}$.^{1,2} By contrast, Li reacts spontaneously to form a complex $\text{Li}\cdot\text{HCl}$, also identified by its EPR spectrum; here the HCl is coordinated side on to the metal atom, which is estimated to bear a charge of $+0.47 e$.³ Insertion of the metal atom M into the H–Cl bond to form the metal hydride HMCl occurs with other metal atoms, notably Al,⁴ Fe,⁵ and Hg.⁶ For example, EPR measurements imply that Al atoms react spontaneously to form the angular divalent species AlCl . The photolability of this and related species probably accounts for the failure to detect HGaCl or HInCl in experiments with Ga or In atoms. Instead, these gave IR evidence of the univalent species MCl ($M = \text{Ga}$ or In) and MH ($M = \text{Ga}$) and the trivalent ones HMCl_2 ($M = \text{Ga}$ or In) and H_2MCl ($M = \text{Ga}$).⁷ HFeCl , formed by the spontaneous reaction of Fe atoms on co-condensation with HCl, has been characterized by its Mössbauer spectrum as well as by the $\nu(\text{Fe}-\text{H})$ mode in its IR spectrum.⁵ While forming a loosely bound complex $\text{Hg}\cdots\text{HCl}$ spontaneously, Hg atoms require photoexcitation before they will insert into the HCl bond to give HHgCl , as identified by IR bands attributable to the $\nu(\text{Hg}-\text{H})$ and $\delta(\text{H}-\text{Hg}-\text{Cl})$ modes.⁶

If Zn and Cd compounds of the type HMCl have not been reported previously and HHgCl has not been studied extensively, the parent compounds MH_2 ^{8–10} and MCl_2 ^{11–13} ($M = \text{Zn}$, Cd , or Hg) have all been investigated in some detail by matrix-isolation methods. In addition, mixed hydride molecules of the types HMOH ($M = \text{Zn}$ or Cd)^{8,14} and CH_3MH ($M = \text{Zn}$, Cd ,

or Hg)^{15,16} have also been described as products of the insertion of the photoexcited metal atoms into the O–H or C–H bonds of H_2O and CH_4 , respectively.

Here, we describe the results of matrix-isolation experiments in which Zn or Cd atoms have been trapped in solid HCl-doped Ar matrixes. The products of any thermal or photolytic changes have been identified by their IR spectra, the conclusions being underpinned by the observed effects of isotopic change (^1H , $^{35,37}\text{Cl}$, and $^{64,66,68}\text{Zn}$) and by reference to the vibrational properties forecast by density functional theory (DFT) calculations. Similar experiments have also been carried out with Hg atoms, and as a result all three vibrational fundamentals of the HHgCl molecule have been identified. The properties of the three HMCl molecules ($M = \text{Zn}$, Cd , or Hg) are compared with those of related metal hydrides, and the mechanism of the insertion reaction leading to them is discussed.

II. Experimental and Theoretical Procedures

Zn (Aldrich, purity 99.999%) and Cd (Aldrich, purity 99.9998%) were each evaporated from a tantalum Knudsen cell that was heated resistively to ca. 300 and 250 °C, respectively, to generate the metal atoms in their electronic ground state. Details of the apparatus have been described previously.¹⁷ Hg atoms were generated simply by heating a reservoir of doubly distilled Hg to 40–50 °C.

The metal vapor produced in this way was co-deposited with an excess of HCl-doped Ar on a CsI window cooled normally to ca. 12 K by means of a Displex closed-cycle refrigerator (Air Products model CS202). The matrix gas, typically with the composition $\text{Ar}:\text{HCl} = 100:2$, was deposited at a rate of 1.0–1.5 mmol h^{-1} over a period of 2 h. The Ar was used as supplied (BOC, Research grade). HCl and DCl (both from Aldrich) were purified before use by fractional condensation in vacuo. Throughout the course of the experiments, problems were experienced with H/D exchange between DCl and the walls of the handling and inlet lines. Attempts were made to minimize this exchange by replacing metal lines and inlets with an all-glass assembly. The apparatus was also conditioned overnight

* To whom correspondence should be addressed. E-mail: T.M.Greene@exeter.ac.uk. Tel.: 0044-(0)1392-263452. Fax.: 0044-(0)1392-263434.

[†] University of Oxford.

[‡] University of Exeter.

by charging it with DCI vapor to a pressure of 50 Torr and then evacuated before proceeding with experiments involving DCI.

After deposition, the IR spectrum of the resulting matrix was recorded. The sample was then exposed to the radiation from a Spectral Energy Hg–Xe arc lamp operating at 800 W. The first step typically involved broad-band UV–vis photolysis ($200 \leq \lambda \leq 800$ nm) with just a water filter to absorb IR radiation and so minimize any heating effects. The effects of more selective photolysis were also investigated using a range of filters: vis-block ($200 \leq \lambda \leq 400$ nm) or interference filters (Oriel) for $\lambda = 313$ nm (full width at half height (fwhh) 16 nm) and $\lambda = 254$ nm (fwhh 10 nm).

IR spectra were recorded, typically at a resolution of 0.5 cm^{-1} and with a wavenumber accuracy of $\pm 0.1 \text{ cm}^{-1}$, using a Nicolet Magna-IR FTIR spectrometer. Measurements in the range $4000\text{--}400 \text{ cm}^{-1}$ were made with a liquid N_2 cooled MCTB detector; measurements at wavenumbers down to 250 cm^{-1} were made with a DTGS detector. UV–vis spectra were recorded in the range $300\text{--}900$ nm using a Perkin-Elmer-Hitachi Model 330 spectrophotometer.

DFT calculations were performed using the GAUSSIAN98 program suite¹⁸ and applying the B3LYP method. The basis set used for calculations involving all three metals was CEP-31G.¹⁹ This set has been shown to give satisfactory results for small molecules of the type discussed here. The specific basis sets were chosen on the basis of giving the closest match to the measured wavenumbers for the symmetrical molecules MH_2 and MCl_2 ($\text{M} = \text{Zn, Cd, or Hg}$).^{8–13} Further theoretical calculations were undertaken using density functional methods of the Amsterdam Density Functional Package (ADF 2002.2).^{20–23} For molecules containing Zn and Hg, triple- ζ accuracy sets of Slater-type orbitals were used, with two polarization functions added. For Cd species, triple- ζ accuracy sets of Slater-type orbitals were used, with a single polarization function added and the cores of the atoms were frozen up to 2p for Cl and 4p for Cd. The local density approximation of Vosko, Wilk, and Nusair²⁴ was used with the nonlocal exchange corrections by Becke²⁵ and nonlocal correlation corrections by Perdew.²⁶ Scalar relativistic corrections were included via the ZORA method. Normal coordinate analysis calculations were carried out using the program ASYM40.²⁷

III. Results

The IR spectra associated with the products of the reactions of Zn, Cd, and Hg atoms with HCl will be reported in turn. Bands have been assigned on the basis of the following criteria: (i) their growth/decay characteristics under different conditions, (ii) comparisons with the spectra registered in control experiments and with the spectra of authentic samples of either a particular species or one related to it, (iii) the observed effects of exchanging H for D or of the naturally occurring isotopes of Cl and Zn, and (iv) consideration of how well the measured spectra are reproduced by the results of DFT calculations. In the experiments with Cd, UV–vis spectra of the matrixes have provided a means of monitoring the fate of the metal atoms²⁸ as well as revealing the growth of a new UV absorption attributable to the HCdCl molecule.

Zinc. When Zn atoms were co-deposited with an excess of Ar doped with 2% HCl at ca. 12 K, the IR spectrum of the deposit contained bands attributable to monomeric HCl and its aggregates^{6,29} as well as weak features associated with trace impurities (H_2O ,³⁰ CO ,³¹ and CO_2)³² that could be kept to a minimum but never wholly eliminated. In addition, the spectrum

TABLE 1: Infrared Absorption Wavenumbers (cm^{-1}) Observed in Solid Ar/HCl/Zn Mixtures or Ar/DCI/Zn Mixtures at 12 K

Zn/HCl	Zn/DCI	assignment
2758.9	2000.7	$\text{Zn}\cdots\text{HCl}$
1957.6	1410.2	HZnCl
1952.3	1406.6	
1948.5	1399.6	
1943.2	1392.6	
1870.8	1357.4	ZnH_2
1821.2	1309.7	HZnZnCl
1817.4	1306.6	
1811.6		
1134.3	728.8	<i>a</i>
956.0		HCl_2^-
696.7		
630.6		ZnH_2
516.9	517.0	ZnCl_2
513.6	513.3	
509.5	509.4	
505.8	505.7	
462.9	462.9	<i>a</i>
449.6	325.5	HZnCl
445.1	321.3	
437.4	317.0	HZnZnCl
431.6	316.3	
424.7	424.0	HZnCl
422.6	421.9	
420.5	420.0	
417.3	416.3	
415.1	413.9	
412.8	<i>b</i>	

^a Unassigned band unshifted by change of metal or isotopic substitution. ^b Too weak for accurate measurement.

revealed a new set of absorptions attributable to a product **1a** that appeared *only* with the co-deposition of Zn vapor; the most prominent feature, which occurred near 2760 cm^{-1} , was accompanied by weaker satellites due either to matrix site effects or to other, distinct products. By reducing the concentration of HCl to 0.1% and so narrowing the absorptions, it was possible clearly to identify a single absorption due to **1a** at 2758.9 cm^{-1} red-shifted by 109.4 cm^{-1} with respect to monomeric HCl. The obvious inference is that **1a** is a weakly bound complex $\text{Zn}\cdots\text{HCl}$, although the perturbation of the HCl thus implied is much greater than that described for “ $\text{Hg}\cdots\text{ClH}$ ” in earlier matrix experiments.⁶ A weak doublet centered near 1586 cm^{-1} in our experiments with Zn atoms must arise from another loosely bound adduct, viz., $\text{Zn}\cdots\text{H}_2\text{O}$, which has been reported previously.³³

Upon photolysis with broad-band UV–vis light ($200 \leq \lambda \leq 800$ nm) for a period of 40 min, the absorption near 2760 cm^{-1} was extinguished and new absorptions were observed to develop, as listed in Table 1 and illustrated in Figure 1. Some of these could be recognized as belonging to known species. Thus, the features at 956.0 and 696.7 cm^{-1} , which gained prominence as the HCl concentration was increased, must correspond to $\nu_1 + \nu_3$ and ν_3 , respectively, of the ClHCl^- anion.^{6,34} Weak bands at 1870.8 and 630.6 cm^{-1} were recognizable as arising from ν_3 and ν_2 , respectively, of the linear ZnH_2 molecule⁸ and a weak quartet at 516.9 , 513.6 , 509.5 , and 505.8 cm^{-1} as arising from ν_3 for different isotopomers of ZnCl_2 .¹¹ In addition, however, photolysis resulted in the appearance and growth of two families of bands which did not correspond to any known product. The first of these, clearly associated with the principal product, **2a**, consisted of multiplets centered near 1950 , 445 , and 420 cm^{-1} . The second, identifiable with a secondary product, **3a**, consisted of two weaker absorptions centered near 1815 and 435 cm^{-1} . The presence of the naturally occurring isotopes ^{35}Cl (75.8%)

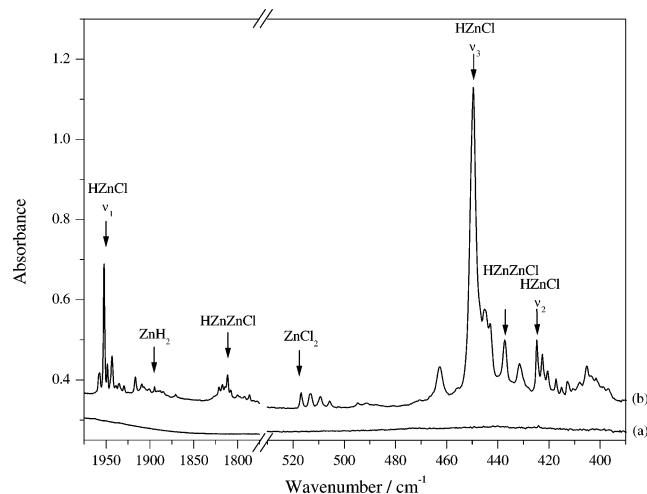


Figure 1. (a) IR spectrum of the deposit formed by co-condensing Zn atoms and 2% HCl in Ar at 12 K. (b) IR spectrum of the same deposit after broad-band UV-vis photolysis.

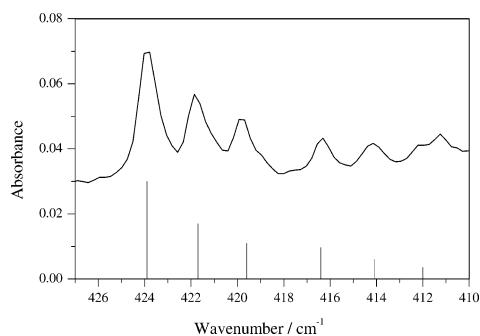


Figure 2. Observed (above) and simulated (below) spectra of the ν_2 mode of DZnCl. The simulated pattern was obtained by assuming a diatomic model for ZnCl and using the observed position for $\nu(^{64}\text{Zn}-^{35}\text{Cl})$.

and ^{37}Cl (24.2%) and ^{64}Zn (48.6%), ^{66}Zn (27.9%), and ^{68}Zn (18.8%)³⁵ undoubtedly contributed to the splitting of some of these absorptions, but matrix site effects needed also to be taken into account. The high-wavenumber bands near 1815 and 1950 cm^{-1} occur in a region characteristic of Zn-H stretching modes (e.g., ZnH_2 1870.2,⁸ CH_3ZnH 1866.1,¹⁵ and HZnOH 1955.0 cm^{-1} ^{8,14}). Moreover, the 420 cm^{-1} band of **2a** was observed to consist of a doublet of triplets (see Figure 2) with the intensities appropriate to a $\nu(\text{Zn}-\text{Cl})$ fundamental.

Changing the conditions of photolysis showed that all the new IR bands described above also appeared after photolysis with near-UV light having $\lambda = 300\text{--}400$ nm, although the reduction in intensity of the photolyzing radiation led to a slower buildup of products. Exposure to visible light ($\lambda = 400\text{--}800$ nm) had no effect on the matrix deposit either before or after UV photolysis. Continued UV irradiation had no effect beyond increasing the intensities of the bands due to **2a**; the bands due to **3a** did not appear to change in intensity.

The experiments were repeated with DCl in place of HCl, with the results included in Table 1. The IR spectrum of the Zn-doped matrix recorded immediately after deposition included a new feature at 2000.7 cm^{-1} correlating with that attributed to the $\text{Zn}\cdots\text{HCl}$ adduct (H/D = 1.3790:1). Broad-band UV-vis irradiation then gave substantial shifts in the wavenumbers of two of the transitions due to **2a**, which was now associated with IR bands near 1400, 420, and 325 cm^{-1} ; the relevant H/D ratios based on the strongest features were thus found to be 1.3880:1, 1.0012–1.0029:1, and 1.3813:1, respectively. Both bands due

TABLE 2: Infrared Absorption Wavenumbers (cm^{-1}) Observed in Solid Ar/HCl/Cd Mixtures or Ar/DCl/Cd Mixtures at 12 K

Cd/HCl	Cd/DCl	assignment
2745.3	1991.4	$\text{Cd}\cdots\text{HCl}$
1839.9	1318.5	HCdCl
1835.8	1317.8	
1832.8	1315.6	
1823.7	1309.2	
1817.0	1304.3	
1813.9	1301.2	
1753.6		CdH_2
1700.4	1221.4	HCdCdCl
1693.8	1212.9	
1688.3		
1142.3	1142.4	<i>a</i>
956.0		HCl_2^-
696.7		
	463.6	<i>a</i>
604.4		CdH_2
601.9		
425.5	306.7	HCdCl
421.8	303.8	
415.3	300.3	
410.7	295.6	HCdCdCl
403.8		
364.5	364.4	HCdCl
357.4	356.7	

^a Unassigned band unshifted by change of metal or isotopic substitution.

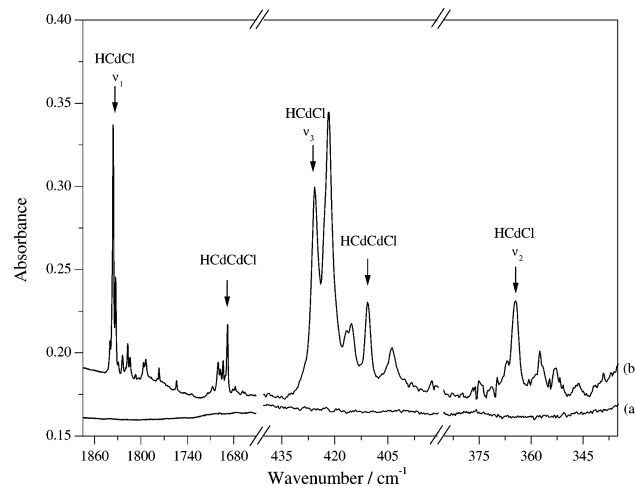


Figure 3. (a) IR spectrum of the deposit formed by co-condensing Cd atoms and 2% HCl in Ar at 12 K. (b) IR spectrum of the same deposit after broad-band UV-vis photolysis.

to **3a** suffered appreciable shifts with H/D ratios of 1.3887:1 and 1.3720:1 for the transitions at high and low wavenumber, respectively.

Cadmium. Similar experiments carried out with Cd atoms gave results analogous in nearly every respect to those described for Zn. Essential details are listed in Table 2; representative spectra are illustrated in Figure 3. In the following account, the results with DCl are given in parentheses. The presence of the metal atoms in the matrix resulted in the appearance of a new IR absorption attributable to the stretching fundamental of a weakly perturbed HCl (DCl) molecule in an initial product **1b**. This occurred at 2745.3 (1991.4) cm^{-1} , i.e., at a slightly lower wavenumber than for the corresponding Zn product **1a**, with H/D = 1.3786:1.

Broad-band UV-vis or UV photolysis led to the decay and disappearance of the IR band due to **1b** and to the appearance of new ones. The main photoproduct, **2b**, was characterized by

TABLE 3: Infrared Absorption Wavenumbers (cm^{-1}) Observed in Solid Ar/HCl/Hg Mixtures or Ar/DCl/Hg Mixtures at 12 K

Hg/HCl	Hg/DCl	assignment
2788.9	2020.4	Hg \cdots HCl
2092.0	1500.5	HHgCl
546.2	393.9	HHgCl
544.2	392.2	
542.8	391.3	
362.8	363.5	HHgCl
354.4	354.6	

strong absorptions occurring at 1832.8 (1318.5), 425.5/421.8 (306.7/303.8), and 364.5 (364.4) cm^{-1} with H/D ratios of 1.3901:1, 1.3873:1/1.3884:1, and 1.0003:1, respectively. A secondary product, **3b**, with properties strongly reminiscent of the Zn compound **3a**, was recognizable by bands near 1693.8 (1212.9) and 410.7 (295.6) cm^{-1} with H/D ratios of 1.3965:1 and 1.3894:1, respectively. By their wavenumbers and response to deuteration, the transitions at 1832.8 and 1693.8 cm^{-1} are most likely to correspond to $\nu(\text{Cd}-\text{H})$ vibrations (cf. CdH_2 1753.5,⁸ CH_3CdH 1760.5,¹⁵ and HCdOH 1836.9 cm^{-1} ^{8,14}). By the same token, the 364.5- cm^{-1} transition of **2b** has the properties expected of a $\nu(\text{Cd}-\text{Cl})$ mode (cf. CdCl_2 327 and 419 cm^{-1} ¹²). In addition to the weak features arising from trace impurities^{30–32} present from the outset of the experiments, the spectrum of the photolyzed matrix included weak absorptions at 1753.6 and 604.4/601.9 cm^{-1} , which can be identified with the formation in low concentration of CdH_2 ;⁸ no corresponding absorption of CdD_2 could be detected, presumably for want of intensity. The possible formation of CdCl_2 was difficult to assess since this molecule absorbs near 420 cm^{-1} ,¹² thereby running the risk of confusion with one of the signals associated with **2b**. However, the experiments with DCl revealed no trace of absorption hereabouts, and so CdCl_2 did not appear to be formed, at least in detectable concentrations. On the other hand, the photoproducts again included the HCl_2^- anion, as evidenced by the appearance of weak bands at 956.0 and 696.7 cm^{-1} ,^{6,34} although with neither Zn nor Cd did experiments give any sign of the corresponding deuterated species.

Selective photolysis revealed that the light with wavelengths near 313 nm was active in promoting the changes described above. Prolonging irradiation with either narrow- or broad-band UV light had no effect beyond increasing the yield of the photoproduct **2b**. The UV–vis spectrum of the condensate immediately after deposition showed an absorption at 312 nm attributable to the $^3\text{P}_1 \leftarrow ^1\text{S}_0$ transition of atomic Cd.²⁸ This absorption was observed to decay on selective UV irradiation of the matrix as the IR spectrum witnessed the appearance and growth of the photoproduct bands. Simultaneously a new feature was observed to develop at 298 nm, originating presumably in the principal product **2b**.

Mercury. Experiments with Hg in place of either Zn or Cd gave results mostly consistent with those reported earlier⁶ (see Table 3 and Figures 4 and 5). There proved, however, to be one significant difference. The IR spectrum of the Hg-doped matrix recorded immediately after deposition included a new band at 2788.9 cm^{-1} red shifted by 79.4 cm^{-1} with respect to free HCl and which decayed rapidly on broad-band UV–vis photolysis. Shifting to 2020.4 cm^{-1} when HCl was replaced by DCl, giving H/D = 1.3804:1, this shows all the signs of originating in a product **1c**, which is almost certainly a complex Hg \cdots HCl analogous to that formed by the lighter Group 12 metal atoms. Curiously, Legay-Sommaire and Legay in their earlier matrix studies of the Hg/HCl system⁶ made no mention

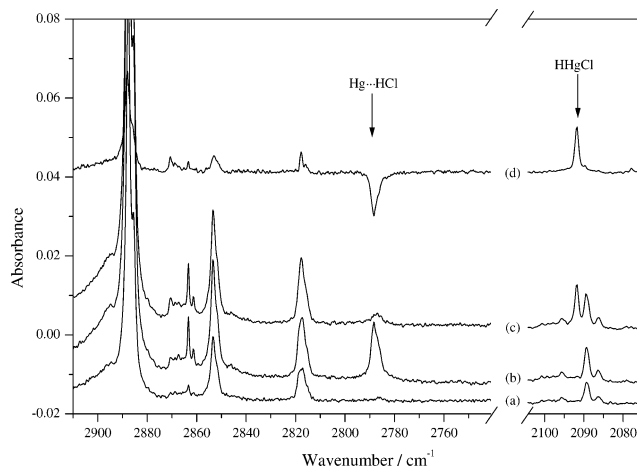


Figure 4. (a) IR spectrum of a deposit formed by condensing 2% HCl in Ar at 12 K. (b) IR spectrum of the deposit formed by co-condensing Hg atoms and 2% HCl in Ar at 12 K. (c) IR spectrum of the Ar/HCl/Hg deposit after broad-band UV–vis photolysis. (d) The IR spectrum displayed in c minus the IR spectrum displayed in b.

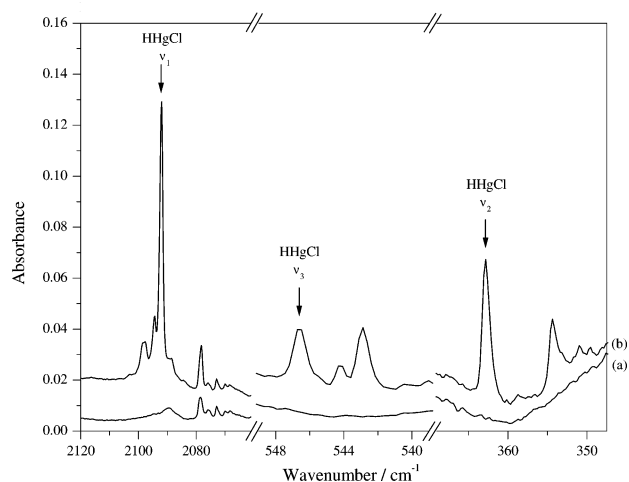


Figure 5. (a) IR spectrum of the deposit formed by co-condensing Hg atoms and 2% HCl in Ar at 12 K. (b) IR spectrum of the same deposit after broad-band UV–vis photolysis.

of this band (which might have been mistaken for the $\nu(\text{H}-\text{Cl})$ mode of an $[\text{HCl}]_n$ oligomer). Instead, they identified a very weakly bound “Hg \cdots ClH” complex with a band red shifted from $\nu(\text{H}-\text{Cl})$ of free HCl by a mere 7.2 cm^{-1} and detectable only in the spectrum of an N_2 matrix with $\text{N}_2:\text{HCl} = 1000:1$.

Either broad-band UV–vis photolysis or selective photolysis near 254 nm of the matrix doped with Hg and HCl resulted not only in the decay of the IR absorption due to **1c** but also in the appearance of an intense IR absorption at 2092.0 cm^{-1} and a weaker matrix-split triplet at 546.2/544.2/542.8 cm^{-1} attributable to a primary product **2c**. In fact, **2c** has been identified previously⁶ as HHgCl, these features representing ν_1 and ν_3 , respectively. In addition, a third absorption not previously reported, but correlating with the other two, was observed to consist of a doublet with components centered at 362.8 and 354.4 cm^{-1} and having relative intensities of 3:1. The corresponding bands in the experiments with DCl occurred at 1500.5 (as reported earlier),⁶ 393.9/392.2/391.3, and 363.5/354.6 cm^{-1} , giving H/D ratios of 1.3942:1, 1.3866/1.3876/1.3872:1, and 0.9981/0.9994:1. There can be little doubt therefore that the third IR band arises from the $\nu(\text{Hg}-\text{Cl})$ fundamental, ν_2 , of the

TABLE 4: Calculated Dimensions (Bond Lengths in Å) of Possible Products of the Reaction between Group 12 Metal Atoms or Dimers and HCl^a

compound	bond	M = Zn	M = Cd	M = Hg
M···HCl ^b	M···H	2.478	2.768	2.561
	H–Cl	1.348	1.342	1.344
M···ClH ^b	M···Cl	4.385	7.015	7.531
	H–Cl	1.328	1.329	1.328
HMCl	H–M	1.156	1.673	1.637
	M–Cl	2.151	2.362	2.398
HMMCl	H–M	1.559	1.720	1.685
	M–M	2.383	2.697	2.683
	M–Cl	2.190	2.408	2.456

^a For details of calculations, see text. ^b Free HCl: H–Cl 1.328 Å.

HHgCl molecule (**2c**) which in its photosynthesis and photolytic properties is plainly analogous to the Zn and Cd species **2a** and **2b**.

Photolysis of these matrixes gave IR spectra that were much simpler than the spectra displayed by the Zn/HCl and Cd/HCl systems under comparable conditions. Thus, there was no sign of bands attributable to the Hg counterpart of **3a** and **3b** or to the known molecules HgH₂¹⁰ and HgCl₂.¹³ Differences in the photolysis conditions of the present and earlier experiments must account for the failure to observe the IR signatures of the HCl₂[−] anion which were reported⁶ to become prominent on photolysis of matrixes with Ar:HCl < 1000:1 at λ = 249 nm using a powerful KrF laser source.

IV. Discussion

The main IR features observed to develop as a result of the reactions induced thermally or photolytically on deposition of Zn, Cd, or Hg atoms (M) in an HCl-doped Ar matrix will be shown to arise from the three products M···HCl (**1a**, **1b**, **1c**), HMCl (**2a**, **2b**, **2c**), and, most probably, HMMCl (**3a**, **3b**). The Hg compound HHgCl (**2c**) has been identified in previous matrix experiments,⁶ and the gaseous complex Hg···HCl, i.e., **1c** (but not Zn···HCl or Cd···HCl), has been characterized in some detail by microwave studies.³⁶

M···HCl [M = Zn (1a), Cd (1b), or Hg (1c)]. The observed IR signatures of each of the products **1a**, **1b**, and **1c** formed on co-deposition of the metal atoms with HCl at low concentrations are wholly consistent with the perturbation of a single HCl molecule by interaction with a metal atom. Analogies with earlier studies involving Hg^{6,36} argue strongly that weakly bound van der Waals complexes of the type M···HCl are formed by Zn and Cd as well as Hg.

DFT calculations find a global minimum for the ground state of such a species with a linear M···HCl geometry and the optimized dimensions given in Table 4. The calculated dimensions for Hg···HCl are in satisfactory agreement with those determined experimentally for the gaseous compounds. Two of the three vibrational fundamentals of the M···HCl or M···ClH adduct are expected to fall below the low-wavenumber threshold of the present IR measurements (250 cm^{−1}), and so the only spectroscopic marker we have in practice is ν₁, the ν(H–Cl) mode. For Zn, Cd, or Hg in an Ar matrix, this was observed to be red shifted with respect to the parent HCl molecule by 109.4, 123.0, or 79.4 cm^{−1}, respectively.

For both M···HCl and M···ClH, the computed wavenumbers for ν₁ show red shifts; the values in the first case (in cm^{−1}) are Zn 276.0, Cd 192.1, and Hg 217.5 cm^{−1} and in the second case Zn 2.8, Cd 0.2, and Hg 0.4 cm^{−1}, as shown in Table 5. Although comparison of the experimental with the theoretical results appears in principle to offer a clear-cut means of deciding

TABLE 5: Comparison of Calculated and Observed Wavenumbers (cm^{−1}) of ν(H–Cl) for Complexes of a Group 12 Metal Atom with HCl (Intensities (km mol^{−1}) Given in Parentheses)

complex		HCl		DCl	
		obs	calc	obs	calc
Zn···HCl ^a	ν(H–Cl)	2758.9	2439.1 (468)	2000.7	1750.6 (238)
	Δν(H–Cl) ^b	−109.4	−276.0	−89.5	196.3
Zn···ClH ^a	ν(H–Cl)		2712.3 (1)		1944.8 (1)
	Δν(H–Cl) ^b		−2.8		2.0
Cd···HCl ^a	ν(H–Cl)	2745.3	2523.0 (370)	1991.4	1810.1 (188)
	Δν(H–Cl) ^b	−123.0	−192.1	−98.8	−136.8
Cd···ClH ^a	ν(H–Cl)		2714.9 (0)		1946.8 (0)
	Δν(H–Cl) ^b		−0.2		−0.1
Hg···HCl ^a	ν(H–Cl)	2788.9	2497.6 (297)	2020.4	1792.3 (151)
	Δν(H–Cl) ^b	−79.4	−217.5	−69.8	−154.6
Hg···ClH ^a	ν(H–Cl)		2714.70 (0)		1946.60 (0)
	Δν(H–Cl) ^b		−0.4		−0.3

^a HCl obs (calc): 2868.3 (2715.1) cm^{−1}; DCl: 2090.2 (1946.9) cm^{−1}.

^b Δν(H–Cl) = ν(H–Cl)_{complex} − ν(H–Cl)_{free}.

whether the matrix species is M···HCl or M···ClH, the issue may be more equivocal in practice when the interaction is only weak. Previous experience³⁷ shows that the wavenumber shift is then liable to change markedly with the move from the gas to the matrix and also from one matrix to another. In the circumstances, however, our experimental results give no reason to believe that the M···HCl adducts adopt a geometry different from the optimum form forecast by the calculations and demonstrated in the gas phase in the case where M = Hg.³⁶ The observed wavenumber shifts Δν(H–Cl) of 79–123 cm^{−1} for M···HCl fall, it should be noted, in the range associated with 1:1 HCl adducts formed by weakly basic molecules. Thus, they may be compared with the corresponding parameters (in cm^{−1} and measured under similar conditions) for 1:1 complexes of HCl with the following species: Xe 13,³⁸ CH₄ 16,³⁹ CO₂ 17,³⁸ ClF 21,⁴⁰ NO 42.5,⁴¹ CO 56,³⁸ C₆H₆ 95,³⁹ HC≡CH 107,³⁹ H₂C=CH₂ 118,³⁹ and CH₃CH=CH₂ 147.³⁹ That the interaction between M and HCl is quite weak is signaled by the UV–vis absorption spectrum measured in the case where M = Cd and where we find that the wavelength of the ³P₁ ← ¹S₀ transition of atomic Cd is quite unaffected by the presence of the HCl in the matrix.^{15,28} In other words, a Group 12 metal atom in its ¹S₀ ground electronic ground-state behaves much like HC≡CH or H₂C=CH₂ in its response to HCl.

It is perfectly possible that the IR absorption 7.2 cm^{−1} red shifted with respect to monomeric HCl reported by Legay-Sommaire and Legay for a solid N₂ matrix⁶ corresponds to the alternative form of the metal atom adduct, viz., Hg···ClH. Certainly the species was found to be photolabile and its decomposition to correlate with the buildup of HHgCl. In no case did our Ar matrixes reveal clear evidence of an analogous feature. It was noticeable, however, that the band apparently associated with the HCl monomer at ca. 2870.5 cm^{−1} did decay appreciably in response to broad-band UV–vis irradiation, and some difference spectra hinted at more than one component to this band.

HMCl [M = Zn (2a), Cd (2b), or Hg (2c)]. As noted previously, the IR bands of **2a** and **2b** near 1950 and 1830 cm^{−1}, respectively, are strongly suggestive of ν(M–H) fundamentals, matching the band of **2c** at 2092.0 cm^{−1} already assigned⁶ to ν(Hg–H) of the HHgCl insertion product. The observed H/D ratios are in keeping with those for other unsymmetrical hydrides of these metals, e.g., CH₃ZnH 1.3877:1,¹⁵ HZnOH 1.3865:1,⁸ CH₃CdH 1.3924:1,¹⁵ and HCdOH 1.3918:1.⁸ **2a**, **2b**, and **2c** are each characterized by two other IR-active transitions at such

TABLE 6: Comparison of Calculated and Observed Wavenumbers (cm⁻¹) for HZnCl (Intensities (km mol⁻¹) Given in Parentheses)

obs		calc ^a		assignment	description of vibrational mode
ν_i	ω_i	DFT	nca		
1952.3	2023.1	1979.8–1978.3	2023.3–2024.3	$\nu_1 (\sigma^+)$	$\nu(\text{Zn-H})$
424.7	424.7	411.1	424.9	$\nu_2 (\sigma^+)$	$\nu(^{64}\text{Zn}-^{35}\text{Cl})$
422.6	422.6	408.9	422.7		$\nu(^{66}\text{Zn}-^{35}\text{Cl})$
420.5	420.5	406.9	420.6		$\nu(^{68}\text{Zn}-^{35}\text{Cl})$
417.3	417.3	403.8	417.4		$\nu(^{64}\text{Zn}-^{37}\text{Cl})$
415.1	415.1	401.6	415.1		$\nu(^{66}\text{Zn}-^{37}\text{Cl})$
412.8	412.8	399.5	413.0		$\nu(^{68}\text{Zn}-^{37}\text{Cl})$
449.6	458.8	423.7–424.4	424.4–456.0	$\nu_3 (\pi)$	$\delta(\text{H-Zn-Cl})$
1406.6	1443.0	1410.4–1411.7	1443.0–1441.7	$\nu_1 (\sigma^+)$	$\nu(\text{Zn-D})$
424.0	424.0	409.8	423.8	$\nu_2 (\sigma^+)$	$\nu(^{64}\text{Zn}-^{35}\text{Cl})$
421.9	421.9	407.7	421.6		$\nu(^{66}\text{Zn}-^{35}\text{Cl})$
420.0	420.0	405.7	419.6		$\nu(^{68}\text{Zn}-^{35}\text{Cl})$
416.3	416.3	402.5	416.3		$\nu(^{64}\text{Zn}-^{37}\text{Cl})$
413.9	413.9	400.3	414.1		$\nu(^{66}\text{Zn}-^{37}\text{Cl})$
<i>b</i>					$\nu(^{68}\text{Zn}-^{37}\text{Cl})$
323.5	330.3	307.8–308.6	331.3–332.1	$\nu_3 (\pi)$	$\delta(\text{D-Zn-Cl})$

^a For details of DFT calculations and nca, see text. $R = \text{Zn-H}$, $r = \text{Zn-Cl}$, $\alpha = \text{H-Zn-Cl}$, $S_1 = \delta R$, $S_2 = \delta r$, $S_3 = \delta \alpha$. Force constant values (in mdyne Å⁻¹) (a) DFT: $F_{11} = 2.2890$; $F_{12} = -0.0187$; $F_{22} = 2.2642$; $F_{33} = 0.2318$. (b) nca: $F_{11} = 2.3966$; $F_{12} = 0.0579$; $F_{22} = 2.4183$; $F_{33} = 0.2686$. ^b Too weak for an accurate measurement.

TABLE 7: Comparison of Calculated and Observed Wavenumbers (cm⁻¹) for HCdCl (Intensities (km mol⁻¹) Given in Parentheses)

obs		calc ^a		assignment	description of vibrational mode
ν_i	ω_i	DFT	nca		
1832.8	1890.0	1861.0	1900.2	$\nu_1 (\sigma^+)$	$\nu(\text{Cd-H})$
364.5	364.5	353.1	364.9	$\nu_2 (\sigma^+)$	$\nu(\text{Cd}-^{35}\text{Cl})$
357.4	357.4	345.7	357.4		$\nu(\text{Cd}-^{37}\text{Cl})$
423.7	432.3	412.2–412.0	431.1–431.0	$\nu_3 (\pi)$	$\delta(\text{H-Cd-Cl})$
1318.5	1352.6	1322.7	1351.9	$\nu_1 (\sigma^+)$	$\nu(\text{Cd-D})$
364.4	364.4	352.6	364.1	$\nu_2 (\sigma^+)$	$\nu(\text{Cd}-^{35}\text{Cl})$
356.7	356.7	345.3	356.5		$\nu(\text{Cd}-^{37}\text{Cl})$
305.3	309.8	297.2–297.0	310.9–310.7	$\nu_3 (\pi)$	$\delta(\text{D-Cd-Cl})$

^a For details of DFT calculations and nca, see text. $R = \text{Cd-H}$, $r = \text{Cd-Cl}$, $\alpha = \text{H-Cd-Cl}$, $S_1 = \delta R$, $S_2 = \delta r$, $S_3 = \delta \alpha$. Force constant values (in mdyne Å⁻¹) (a) DFT: $F_{11} = 2.0375$; $F_{12} = -0.0370$; $F_{22} = 1.9650$; $F_{33} = 0.2713$; (b) nca: $F_{11} = 2.1204$; $F_{12} = -0.2073$; $F_{22} = 2.1227$; $F_{33} = 0.2968$.

TABLE 8: Comparison of Calculated and Observed Wavenumbers (cm⁻¹) for HHgCl (Intensities (km mol⁻¹) Given in Parentheses)

obs		calc ^a		assignment	description of vibrational mode
ν_i	ω_i	DFT	nca		
2092.0	2167.9	2036.1	2169.3	$\nu_1 (\sigma^+)$	$\nu(\text{Hg-H})$
362.8	362.8	338.7	363.1	$\nu_2 (\sigma^+)$	$\nu(\text{Hg}-^{35}\text{Cl})$
354.4	354.4	330.8	354.6		$\nu(\text{Hg}-^{37}\text{Cl})$
544.4	555.5	487.6–487.5	555.6–555.5	$\nu_3 (\pi)$	$\delta(\text{H-Hg-Cl})$
1500.5	1539.1	1444.0	1538.2	$\nu_1 (\sigma^+)$	$\nu(\text{Hg-D})$
363.5	363.5	338.5	363.0	$\nu_2 (\sigma^+)$	$\nu(\text{Hg}-^{35}\text{Cl})$
354.6	354.6	330.6	354.5		$\nu(\text{Hg}-^{37}\text{Cl})$
392.5	398.2	349.5–349.3	398.3–398.0	$\nu_3 (\pi)$	$\delta(\text{D-Hg-Cl})$

^a For details of DFT calculations and nca, see text. $R = \text{Hg-H}$, $r = \text{Hg-Cl}$, $\alpha = \text{H-Hg-Cl}$, $S_1 = \delta R$, $S_2 = \delta r$, $S_3 = \delta \alpha$. Force constant values (in mdyne Å⁻¹) (a) DFT: $F_{11} = 2.4491$; $F_{12} = -0.0199$; $F_{22} = 2.0140$; $F_{33} = 0.3683$. (b) nca: $F_{11} = 2.7810$; $F_{12} = 0.0770$; $F_{22} = 2.3165$; $F_{33} = 0.4782$.

lower wavenumbers. One of these, near 445 (**2a**), 422 (**2b**), or 544 cm⁻¹ (**2c**), shifts appreciably on deuteration with H/D ratios of 1.38–1.39:1, whereas the other is virtually unaffected by this change but shows a splitting with wavenumbers and relative intensities clearly implying a major excursion by a single Cl atom. Accordingly, the first bears all the hallmarks of a $\delta(\text{H-M-Cl})$ vibration, whereas the second must surely be associated with a $\nu(\text{M-Cl})$ vibration. Hence all three fundamentals have now been located for each of the molecules HZnCl, HCdCl, and HHgCl as formed in an Ar matrix.

Unsurprisingly, DFT calculations find a linear equilibrium geometry with $C_{\infty v}$ symmetry for each of these molecules; the

dimensions are given in Table 4. The wavenumbers, isotopic shifts, and relative intensities of the IR absorptions observed for the matrix-isolated molecules are found to be in generally close agreement with the properties predicted by the calculations for the optimized ground states of the species, as shown in Tables 6–8. Admittedly, the level of agreement falls somewhat in the case where $M = \text{Hg}$, undoubtedly as a result of failings of the calculations, for example, in taking proper accounts of relativistic effects, but the correlation between observed and computed properties is invariably close enough to support the identification of the linear molecule HMCl molecule for $M = \text{Zn, Cd, or Hg}$.

TABLE 9: Comparison of Calculated and Observed Wavenumbers (cm⁻¹) for HMMCl (Intensities (km mol⁻¹) Given in Parentheses)

metal	assignment	description of mode	HCl		DCl	
			obs	calc	obs	calc
Zn	$\nu_1(\sigma^+)$	$\nu(\text{Zn-H})$	1811.6	1875.0 (349)	1308.2	1336.3 (179)
	$\nu_2(\sigma^+)$	$\nu(\text{Zn-Cl})$	<i>a</i>	396.6 (61)	<i>a</i>	396.5 (61)
	$\nu_3(\sigma^+)$	$\nu(\text{Zn-Zn})$	<i>a</i>	207.8 (9)	<i>a</i>	206.9 (8)
	$\nu_4(\pi)$	$\delta(\text{Zn-Zn-H})$	437.4	384.4 (39)	316.7	280.2 (18)
	$\nu_5(\pi)$	$\delta(\text{Zn-Zn-Cl})$	<i>a</i>	68.5 (7)	<i>a</i>	67.5 (7)
Cd	$\nu_1(\sigma^+)$	$\nu(\text{Cd-H})$	1688.3	1708.1 (417)	1217.2	1213.6 (221)
	$\nu_2(\sigma^+)$	$\nu(\text{Cd-Cl})$	<i>a</i>	334.1 (62)	<i>a</i>	334.1 (62)
	$\nu_3(\sigma^+)$	$\nu(\text{Cd-Cd})$	<i>a</i>	157.9 (4)	<i>a</i>	157.6 (4)
	$\nu_4(\pi)$	$\delta(\text{Cd-Cd-H})$	407.3	363.2 (40)	295.6	260.8 (19)
	$\nu_5(\pi)$	$\delta(\text{Cd-Cd-Cl})$	<i>a</i>	63.4 (6)	<i>a</i>	63.1 (6)
Hg ^b	$\nu_1(\sigma^+)$	$\nu(\text{Hg-H})$		1872.2 (548)		1327.6 (276)
	$\nu_2(\sigma^+)$	$\nu(\text{Hg-Cl})$		311.1 (67)		311.0 (67)
	$\nu_3(\sigma^+)$	$\nu(\text{Hg-Hg})$		142.8 (3)		142.6 (3)
	$\nu_4(\pi)$	$\delta(\text{Hg-Hg-H})$		425.2 (10)		303.8 (5)
	$\nu_5(\pi)$	$\delta(\text{Hg-Hg-Cl})$		64.8 (4)		64.6 (4)

^a Band presumed to be too weak, too low in wavenumber, or too close to that of a more abundant species to be observed. ^b The species HHgHgCl was not detected.

Normal coordinate analysis calculations have been carried out for each of the molecules HMCl with the dimensions taken from the DFT-calculated structure as detailed in Table 4. The observed wavenumbers for the fundamentals have been harmonized using two anharmonicity constants x_i , where $\nu_i = \omega_i(1 - x_i)$; these are $x_i = 0.035$ for M-H stretching and $x_i = 0.020$ for HMCl angle deformation. For the deuterated species, Dennison's rule⁴² was applied such that $x_i' = x_i\nu'/\nu_i$. Such an approach has proved successful in the analysis of the vibrational spectra of [H₂GaCl]₂,⁴³ HInCl₂,⁷ and H₂InCl.⁷ The symmetry coordinates used in the refinement are given in Tables 6–8, along with the values obtained for the force constants. To allow for comparison, the Cartesian force constants given by the DFT calculations have been transformed to a set of constants corresponding to the symmetry coordinates. Comparison of the M-H stretching force constants of the HMCl molecules, as determined by the normal coordinate analysis (nca) treatment, shows that they are consistently somewhat larger than those deduced for the symmetrical HMM molecules^{8,10} (cf. the following values in mdy \AA^{-1} in the order HMCl/HMH: Zn 2.40/2.20; Cd 2.12/1.95; Hg 2.78/2.40). By contrast, the M-Cl stretching force constants are consistently somewhat smaller than in the corresponding CIMCl molecules^{11–13} (with values in mdy \AA^{-1} in the order HMCl/CIMCl: Zn 2.42/2.55; Cd 2.12/2.24; Hg 2.32/2.60). Such a pattern is expected on the basis of the trans influence of the H and Cl ligands,⁴⁴ reflecting the different abilities of their valence orbitals to interact with the np_z valence orbital of the central metal atom and leading to more or less polar M-X bonds (X = H or Cl).

HMMCl [M = Zn (3a) and Cd (3b)]. No more than two IR transitions could be ascribed to each of the secondary photoproducts **3a** and **3b**, the formation of which is favored by raising the metal concentration and/or the temperature of deposition. These features, allied to analogies with earlier matrix studies involving Zn and Cd vapors, suggest that **3a** and **3b** are dimetallic products containing an M₂ core (cf. HZnZnH, ZnZnH, and CdCdH).⁸ The wavenumbers and H/D ratios of the two absorptions imply that they arise from the stretching and bending of an M-H fragment, and the magnitude of the H/D ratio for the absorption at lower wavenumber makes it clear that the M-H fragment is tethered to a relatively massive atom. Neither by their vibrational nor by their photolytic properties are **3a** and **3b** recognizable as any dimetal species characterized earlier;

unlike HZnZnH, ZnZnH, and CdCdH,⁸ for example, they show no signs of being photolabile on exposure to broad-band UV-vis radiation. In the circumstances, the most likely interpretation is that the new compounds are HZnZnCl and HcdCdCl, formed presumably by insertion of the metal dimer into the H-Cl bond since at no stage did the spectra bear any trace of the diatomic species MH⁸ and MCl.^{45,46}

DFT calculations have identified a global minimum corresponding to an equilibrium geometry for each of the HMMCl molecules (M = Zn, Cd, or Hg). The dimensions and vibrational properties determined in this way are given in Tables 4 and 9, respectively. Of the three fundamentals expected to appear in IR absorption at wavenumbers between 2000 and 250 cm⁻¹, only two show a marked response to deuteration, viz., the $\nu(\text{M-H})$ [$\nu_1(\sigma^+)$] and $\delta(\text{M-M-H})$ [$\nu_4(\pi)$] modes; the third corresponds to the $\nu(\text{M-Cl})$ fundamental [$\nu_2(\sigma)$]. The stretching modes ν_1 and ν_2 are each computed to occur at appreciably lower wavenumber than the corresponding modes of HMCl. Comparison of the observed with the simulated spectra then makes a plausible case for identifying **3a** with HZnZnCl and **3b** with HcdCdCl.

Mechanism of Insertion. Earlier experiments^{8,14,15,47} and theoretical⁴⁷ studies have shown that Group 12 metal atoms in their ¹S ground electronic state are not capable of inserting spontaneously into H-H, C-H, or Si-H bonds. By contrast, excitation to the ¹P state does allow for spontaneous reaction; whether excitation to the lower-lying ³P state also results in reaction appears, though, to depend on the substrate (e.g., H₂ or CH₄)⁴⁷ and whether the interaction occurs in the gas or matrix phases.^{15,48} Irradiation giving the ³P₁ metal excited state certainly promotes insertion into the bonds of H₂,⁸ CH₄,¹⁵ or SiH₄⁴⁹ when the relevant species are isolated together in a solid Ar matrix.

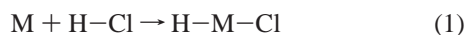
HCl has a dissociation energy close to that of H₂ and to the mean bond energy of C-H in the CH₄ molecule,^{49,50} but by virtue of the increased energy of the polar metal-chlorine bonds, it offers energetically a more favorable opportunity for metal insertion than does either H₂ or CH₄. According to our calculations (see Table 10), the energy change for reaction 1 involving a group 12 metal atom M in its ground electronic state is estimated to be -126, -71, and -4 kJ mol⁻¹ for M = Zn, Cd, and Hg, respectively, results in keeping with expectations based on known or calculated mean bond energy

TABLE 10: Comparison of the Energies (in kJ mol⁻¹) of the Possible Products of the Reaction between a Group 12 Metal Atom and HCl^a

compound	M = Zn	M = Cd	M = Hg
M \cdots HCl	-5.07	-4.92	-3.69
M \cdots ClH	+9 \times 10 ⁻³	+1 \times 10 ⁻²	+1 \times 10 ⁻²
HMCl (³ A')	+203 ^c	+206 ^c	+312 ^c
HMCl (¹ Σ^+)	-126	-71	-4
M (³ P)	+410 ^a /391 ^b	+385 ^a /374 ^b	+495 ^a /500 ^b

^a Basis set CEP-31G. ^b Experimental value, see ref 28. ^c Values derived from the energy difference between HMCl (¹ Σ^+) and HMCl (³A') determined by ADF calculations (for details, see text) and the GAUSSIAN98 estimate for the formation energy of HMCl (¹ Σ^+).

terms;^{8,50} the corresponding reactions with H₂ and CH₄ are consistently endoergic.^{8,15} Although a spontaneous reaction



between Hg and HCl does not occur, as previously attested by experiment,⁶ Zn and Cd atoms are potentially more reactive. In any event, a solid matrix environment that includes a dopant is always liable to influence the chemistry of an atom, as well as trapping out reaction products formed prior to, or during, condensation. Accordingly, one of our first concerns was to investigate the possibility of any thermally induced reaction between a Group 12 metal atom and HCl.

Of insertion there is no trace, however, under the conditions of our experiments. Instead, enforced proximity of M atoms and HCl molecules gives rise to a weakly bound van der Waals complex, on the evidence of a red shift of the $\nu(\text{H}-\text{Cl})$ vibration amounting to 79–123 cm⁻¹. The preferred form of such a pair has a linear M \cdots HCl configuration, as deduced from the microwave spectrum of the gaseous Hg complex,³⁶ although our calculations indicate that there is little to choose energetically between this and the alternative linear arrangement M \cdots ClH. Just as the HCl molecule suffers relatively minor perturbation, so the M atom appears from its ³P₁ \leftarrow ¹S₀ UV transition to respond imperceptibly to the interaction.

On the other hand, it is clear from our experiments, and from earlier experiments with Hg atoms,⁶ that photoexcitation of the atoms to the ³P₁ state leads to insertion into the H–Cl bond with the formation of HMCl. The ³P₁ \leftarrow ¹S₀ electronic transition has been recorded for Zn or Cd atoms isolated in Ar matrixes.²⁸ For Zn, this transition appears as a weak doublet at 295/298 nm, while Cd atoms give rise to a weak, asymmetric doublet at 311/313 nm, which we observe as a single band at 312 nm in the UV–vis spectrum of the deposit. Our experiments have shown that HZnCl is formed following irradiation with $\lambda = 300\text{--}400$ nm and that HCdCl is formed on irradiation with light near 313 nm. It seems likely that excitation to the more energetic ¹P₁ excited state of the metal atoms is also able to effect this change. The ¹P₁ \leftarrow ¹S₀ transition for Zn, Cd, and Hg atoms isolated in Ar matrixes gives rise to strong bands at 207, 220, and 179 nm, respectively.²⁸ The formation of HMCl upon broad-band photolysis may well involve reactions of Zn and Cd in their ¹P₁ excited states, but for Hg atoms, this transition lies well beyond the atmospheric cutoff. Only under matrix conditions does insertion emerge as the reaction channel favored by the M (³P) atoms: in the gas phase, energy transfer from the excited atoms is normally followed by isomerization or elimination reactions of the substrate, where these are energetically feasible.⁵¹ Earlier matrix studies have established that M (³P) inserts (i) into an H–X bond to give the photostable singlet product H–M–X, with a linear H–M–X skeleton, where M = H,⁸ CH₃,¹⁵ or SiH₃,⁴⁹ and (ii) into a carbon–halogen bond

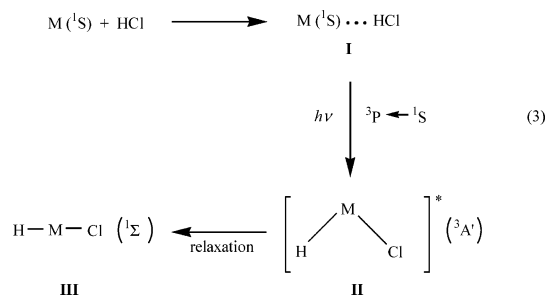
of a saturated or unsaturated halocarbon.⁵² On the face of it, the reactions are opposed by virtually no activation barrier ($RT < 0.2$ kJ mol⁻¹ at 10–20 K), but the slight blue shifts observed for the ³P \leftarrow ¹S₀ absorptions imply access to extra energy that would be sufficient to overcome a barrier in the order of 15 kJ mol⁻¹.¹⁵ In the gas phase, M (³P) atoms react with HX molecules, where X = H or SiH₃, in accordance with eq 2⁴⁷



Accurate quantum-state-resolved distributions, determined for the vibrational and rotational energy of the MH (ν, N) fragment, point to a mechanism in which the excited M atom inserts into the H–X bond with little or no activation barrier to form a triplet intermediate [H–M–X]* with an angular skeleton and an M–H bond distance close to that of the final diatomic product MH. The gaseous intermediate is apparently too short lived for statistical population of all degrees of freedom and is liable to decompose within one H–M–X bending vibration. According to ab initio calculations on the M (³P)/H₂ system, a side-on approach of the H₂ molecule with only slight H–H bond stretching is initially favored; the potential energy drops continuously as M approaches H₂, leading to a local minimum in the PE surface at fairly short M \cdots H₂ separations (1.8–2.0 Å). There is then a slight rise in PE before the H–H bond suddenly breaks, and the H–M–H bond angle increases sharply to ca. 70°, yielding a second local minimum in the PE surface. Another slight rise in PE then opposes the decomposition of this intermediate into H + MH. In the analogous reaction with CH₄ (i.e., X = CH₃), however, the progress of the reaction M (³P) \cdots CH₄ \rightarrow [CH₃MH]* is inhibited by a substantial barrier attributable to steric factors.⁴⁷

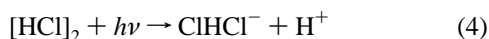
For the reaction between a Group 12 metal atom and HCl, our calculations were unable to locate any minima for a complex formed between the metal atom in its ³P₁ excited state and the HCl molecule. They therefore suggest that excitation to the ³P state allows for spontaneous insertion into the H–Cl bond to give the ³A' excited state of the HMCl molecule, **II**. These excited states lie 329, 277, and 316 kJ mol⁻¹ above the linear ground state for M = Zn, Cd, and Hg, respectively. The excited state then relaxes to afford the linear ground-state molecule, HMCl, **III**, as shown in eq 3. As well as holding the initial reagents together for many collisions, the matrix cage fulfills the vital role of retaining the triplet intermediate **II**, inhibiting its fragmentation and also providing an energy reservoir that permits the thermal relaxation of **II** to its linear, singlet ground state **III**. This ability of a solid matrix to confine reagents and intermediates and so favor reaction pathways that are otherwise avoided is already familiar,⁴⁸ being well exemplified by the matrix isolation experiments leading to the first sighting of HArF⁵³ and of the chlorine oxides ClOCl, ClClO₂, and ClOCIO.⁵⁴ On the other hand, it is still not clear how the activation barrier believed to oppose the insertion of M (³P) into a C–H bond of CH₄ is successfully surmounted in an Ar matrix.¹⁵ One possibility is that the M (³P) \cdots CH₄ complex is sufficiently long lived to absorb a second photon and so be further excited into a state possessing enough energy to overcome the barrier to insertion. In the absence of further information, we cannot of course rule out the possibility that **2** is also photolabile and that photoexcitation is not necessarily confined simply to the creation of M (³P) atoms. The change from a triplet to a singlet state may, for example, depend on a formally forbidden electronic transition of **2** which can be induced under the conditions of relatively broad-band photolysis used in the present experiments. There is clearly scope for

further studies with photolyzing radiation whose wavelength is much more closely defined.



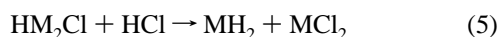
The secondary products **3a** and **3b**, which we believe to be HZnZnCl and HCdCdCl, respectively, are almost certainly formed by processes similar to those set out in eq 3 but now involve the metal dimer M_2 . The failure to observe any IR signal attributable to the species MH,⁸ MCl,⁴⁵ HMMH,⁸ or CIMMCl would appear to rule out the possibility that these products are formed by association of MH and MCl fragments. Although the Group 12 metal atoms form only very weakly bound aggregates, the matrixes produced by condensation of Zn or Cd vapor with Ar or Kr at 10–12 K have been shown previously by their UV–visible absorption²⁸ and Raman⁵⁵ spectra to contain a fraction of the relevant dimers. The formation of dizinc and dicadmium species analogous to **3a** and **3b** has also been observed on isolation of the metal vapors from a microwave discharge source in a H_2 -doped Ar matrix.⁸ Interestingly, though, there is no sign of Hg_2 species in either the present or earlier experiments,^{6,10} suggesting that metal dimers are not trapped in significant concentrations in this case.

The only other secondary photoproduct of significance in the present context is the ClHCl^- anion, the yield of which becomes appreciable only in the experiments with Zn and Cd, and then at higher HCl concentrations. As suggested previously,⁶ it is likely that ClHCl^- is produced by the metal-mediated photodissociation of the HCl dimer (eq 4)



Irradiation of HCl in a metal-free Ar matrix at $\lambda = 193$ nm has been shown⁵⁶ to give rise to ClHCl^- and ArHAr^+ . Our matrixes were not exposed to radiation of significant power at wavelengths shorter than ca. 250 nm, and the IR spectra gave no hint of absorptions attributable to the ArHAr^+ cation. In the circumstances, the cation MH^+ ($\text{M} = \text{Zn}$ or Cd) might be expected to complement the formation of ClHCl^- , but there was no obvious IR signal answering to this species⁸ either (which might be expected in any case to suffer photobleaching in our experiments).⁵⁷

Finally, experiments involving Zn or Cd atoms also revealed the formation of MH_2 and MCl_2 ($\text{M} = \text{Zn}$ or Cd). In matrixes containing a very low concentration of HCl, however, these products were not detected, nor are the corresponding species formed when Hg atoms react with HCl. This suggests that the formation of MH_2 and MCl_2 may involve the reaction of HM_2Cl with a further molecule of HCl, as shown in eq 5



V. Conclusions

A study of the reaction between Zn, Cd, or Hg atoms and HCl molecules has been carried out using the technique of matrix isolation. Hence it has been shown that, upon co-

condensation of the metal atoms and HCl, an adduct $\text{M} \cdots \text{HCl}$ is first formed. Following photoexcitation of the metal, this reacts to give the linear insertion species HMCl. In addition, the species HMMCl ($\text{M} = \text{Zn}$ or Cd) are also formed by reaction of the metal dimers with HCl. The reaction products have been characterized by their IR spectra supported by the results of normal coordinate analysis and DFT calculations. The mechanism of the insertion process, investigated using filtered photolysis, involves excitation of the metal atoms to the ${}^3\text{P}$ excited electronic state.

Acknowledgment. The authors thank the EPSRC for financial support, including the funding of a studentship for V.A.M.

References and Notes

- (1) Davies, M. A.; Lindsay, D. M. *Surf. Sci.* **1985**, *156*, 335.
- (2) Lindsay, D. M.; Symons, M. C. R.; Herschbach, D. R.; Kwiram, A. L. *J. Phys. Chem.* **1982**, *86*, 3789.
- (3) Kasai, P. H. *J. Phys. Chem. A* **2000**, *104*, 4514.
- (4) Köppe, R.; Kasai, P. H. *J. Am. Chem. Soc.* **1996**, *118*, 135.
- (5) Parker, S. F.; Peden, C. H. F.; Barrett, P. H.; Pearson, R. G. *J. Am. Chem. Soc.* **1984**, *106*, 1304.
- (6) (a) Legay-Sommaire, N.; Legay, F. *Chem. Phys. Lett.* **1999**, *314*, 40. (b) Legay-Sommaire, N.; Legay, F. *J. Phys. Chem.* **1995**, *99*, 16945.
- (7) Himmel, H.-J.; Downs, A. J.; Greene, T. M. *J. Am. Chem. Soc.* **2000**, *122*, 922.
- (8) Greene, T. M.; Brown, W.; Andrews, L.; Downs, A. J.; Chertihin, G. V.; Runeberg, N.; Pykkö, P. *J. Phys. Chem.* **1995**, *99*, 7925.
- (9) Xiao, Z. L.; Hauge, R. H.; Margrave, J. L. *High Temp. Sci.* **1991**, *31*, 59.
- (10) Legay-Sommaire, N.; Legay, F. *Chem. Phys. Lett.* **1993**, *207*, 123.
- (11) (a) Loewenschuss, A.; Ron, A.; Schnepf, O. *J. Chem. Phys.* **1968**, *49*, 272. (b) Beattie, I. R.; Jones, P. J.; Young, N. A. *Chem. Phys. Lett.* **1991**, *177*, 579.
- (12) (a) Loewenschuss, A.; Ron, A.; Schnepf, O. *J. Chem. Phys.* **1969**, *50*, 2502. (b) Strull, A.; Givan, A.; Loewenschuss, A. *J. Mol. Spectrosc.* **1976**, *62*, 283. (c) Given, A.; Loewenschuss, A. *Spectrochim. Acta* **1978**, *34A*, 765.
- (13) (a) Givan, A.; Loewenschuss, A. *J. Chem. Phys.* **1976**, *64*, 1967. (b) Givan, A.; Loewenschuss, A. *J. Chem. Phys.* **1976**, *65*, 1851.
- (14) Macrae, V. A.; Greene, T. M.; Downs, A. *J. Phys. Chem. Chem. Phys.* in press.
- (15) Greene, T. M.; Andrews, L.; Downs, A. *J. Am. Chem. Soc.* **1995**, *117*, 8180.
- (16) Legay-Sommaire, N.; Legay, F. *Chem. Phys.* **1996**, *211*, 367.
- (17) Himmel, H.-J.; Downs, A. J.; Greene, T. M.; Andrews, L. *Organometallics* **2000**, *19*, 1060.
- (18) Frisch, M. J.; Trucks, G. W.; Schlegel, H. B.; Scuseria, G. E.; Robb, M. A.; Cheeseman, J. R.; Zakrzewski, V. G.; Montgomery, J. A., Jr.; Stratmann, R. E.; Burant, J. C.; Dapprich, S.; Millam, J. M.; Daniels, A. D.; Kudin, K. N.; Strain, M. C.; Farkas, O.; Tomasi, J.; Barone, V.; Cossi, M.; Cammi, R.; Mennucci, B.; Pomelli, C.; Adamo, C.; Clifford, S.; Ochterski, J.; Petersson, G. A.; Ayala, P. Y.; Cui, Q.; Morokuma, K.; Malick, D. K.; Rabuck, A. D.; Raghavachari, K.; Foresman, J. B.; Cioslowski, J.; Ortiz, J. V.; Stefanov, B. B.; Liu, G.; Liashenko, A.; Piskorz, P.; Komaromi, I.; Gomperts, R.; Martin, R. L.; Fox, D. J.; Keith, T.; Al-Laham, M. A.; Peng, C. Y.; Nanayakkara, A.; Gonzalez, C.; Challacombe, M.; Gill, P. M. W.; Johnson, B. G.; Chen, W.; Wong, M. W.; Andres, J. L.; Head-Gordon, M.; Replogle, E. S.; Pople, J. A. *Gaussian 98*; Gaussian, Inc.: Pittsburgh, PA, 1998.
- (19) Stevens, W. J.; Krauss, M.; Basch, H.; Jasien, P. G. *Can. J. Chem.* **1992**, *70*, 612.
- (20) Baerends, E. J.; Ellis, D. E.; Ros, P. *Chem. Phys.* **1973**, *2*, 41.
- (21) Versluis, L.; Ziegler, T. *J. Chem. Phys.* **1988**, *88*, 322.
- (22) te Velde, G.; Baerends, E. J. *J. Comput. Phys.* **1992**, *99*, 84.
- (23) Fonseca Guerra, C.; Snijders, J. G.; te Velde, G.; Baerends, E. J. *Theor. Chem. Acc.* **1998**, *99*, 391.
- (24) Vosko, S. H.; Wilk, L.; Nusair, M. *Can. J. Phys.* **1980**, *58*, 1200.
- (25) Becke, A. D. *Phys. Rev.* **1988**, *A38*, 3098.
- (26) Perdew, J. P. *Phys. Rev.* **1986**, *B33*, 8822; **1986**, *B34*, 7046.
- (27) Hedberg, L.; Mills, I. M. ASYM40, version 3.0, update of program ASYM20. *J. Mol. Spectrosc.* **1993**, *160*, 117.
- (28) (a) Ault, B. S.; Andrews, L. *J. Mol. Spectrosc.* **1977**, *65*, 102. (b) Laursen, S. L.; Cartland, H. E. *J. Chem. Phys.* **1991**, *95*, 4751.
- (29) (a) Maillard, D.; Schriver, A.; Perchard, J. P.; Girardet, C.; Robert, D. *J. Chem. Phys.* **1977**, *67*, 3917. (b) Maillard, D.; Schriver, A.; Perchard,

J. P.; Girardet, C. *J. Chem. Phys.* **1979**, *71*, 505, 517. (c) Girardet, C.; Maillard, D.; Schriver, A.; Perchard, J. P. *J. Chem. Phys.* **1979**, *70*, 1511.

(30) (a) Ayers, G. P.; Pullin, A. D. E. *Spectrochim. Acta* **1976**, *32A*, 1629. (b) Fredin, L.; Nelander, B.; Ribbegård, G. *J. Chem. Phys.* **1977**, *66*, 4065.

(31) (a) Fredin, L.; Nelander, B.; Ribbegård, G. *J. Mol. Spectrosc.* **1974**, *53*, 410. (b) Guasti, R.; Schettino, V.; Brigot, N. *Chem. Phys.* **1978**, *34*, 391.

(32) Dubost, H. *Chem. Phys.* **1976**, *12*, 139.

(33) Kauffman, J. W.; Hauge, R. H.; Margrave, J. L. *J. Phys. Chem.* **1985**, *89*, 3541.

(34) Jacox, M. E. *J. Phys. Chem. Ref. Data* **1998**, *27*, 157 and references therein.

(35) *CRC Handbook of Chemistry and Physics*, 83rd ed.; Lide, D. R., Ed.; CRC Press: Boca Raton, FL, 2002–2003.

(36) Shea, J. A.; Campbell, E. J. *J. Chem. Phys.* **1984**, *81*, 5326.

(37) See, for example, dihalogen...CO complexes: Schriver, A.; Schriver-Mazzuoli, L.; Chaquin, P.; Bahou, M. *J. Phys. Chem. A* **1999**, *103*, 2624.

(38) Fourati, N.; Silvi, B.; Perchard, J. P. *J. Chem. Phys.* **1984**, *81*, 4737.

(39) Barnes, A. J. *J. Mol. Struct.* **1983**, *100*, 259.

(40) Andrews, L.; Hunt, R. D. *J. Chem. Phys.* **1988**, *89*, 3502.

(41) de Saxce, A.; Sanna, N.; Schriver, A.; Schriver-Mazzuoli, L. *Chem. Phys.* **1994**, *185*, 365.

(42) (a) Dennison, D. M. *Rev. Mod. Phys.* **1940**, *12*, 175. (b) Hansen, G. E.; Dennison, D. M. *J. Chem. Phys.* **1952**, *20*, 313.

(43) Pulham, C. R.; Downs, A. J.; Goode, M. J.; Greene, T. M.; Mills, I. M. *Spectrochim. Acta* **1995**, *51A*, 769.

(44) See, for example: Housecroft, C. E.; Sharpe, A. G. *Inorganic Chemistry*; Prentice Hall: Harlow, U.K., 2001.

(45) Givan, A.; Loewenschuss, A. *J. Mol. Struct.* **1982**, *78*, 299.

(46) Huber, K. P.; Herzberg, G. *Molecular Spectra and Molecular Structure. IV. Constants of Diatomic Molecules*; van Nostrand Reinhold: New York, 1979.

(47) Breckenridge, W. H. *J. Phys. Chem.* **1996**, *100*, 14840.

(48) Himmel, H.-J.; Downs, A. J.; Greene, T. M. *Chem. Rev.* **2002**, *102*, 4191.

(49) Macrae, V. A.; Greene, T. M.; Downs, A. J. *J. Phys. Chem. A*, **2004**, *108*, 1393.

(50) Huheey, J. E.; Keiter, E. A.; Keiter, R. L. *Inorganic Chemistry: Principles of Structure and Reactivity*, 4th ed.; HarperCollins: New York, 1993.

(51) (a) Breckenridge, W. H.; Umemoto, U. *Adv. Chem. Phys.* **1982**, *50*, 325. (b) Breckenridge, W. H. In *Reactions of Small Transient Species: Kinetics and Energetics*; Fontijn, A., Clyne, M. A. A., Eds.; Academic Press: London, 1983; p 157.

(52) (a) Cartland, H. E.; Pimentel, G. C. *J. Phys. Chem.* **1986**, *90*, 1822.

(b) Cartland, H. E.; Pimentel, G. C. *J. Phys. Chem.* **1989**, *93*, 8021.

(53) Khriachtchev, L.; Pettersson, M.; Runeberg, N.; Lundell, J.; Räsänen, M. *Nature* **2000**, *406*, 874.

(54) Jacobs, J.; Kronberg, M.; Müller, H. S. P.; Willner, H. *J. Am. Chem. Soc.* **1994**, *116*, 1106.

(55) Givan, A.; Loewenschuss, A. *Chem. Phys. Lett.* **1979**, *62*, 592.

(56) Räsänen, M.; Seetula, J.; Kunttu, H. *J. Chem. Phys.* **1993**, *98*, 3914.

(57) Andrews, L. *Annu. Rev. Phys. Chem.* **1979**, *30*, 79.